Third-body formation by selective transfer in a NiCr / AgPd electrical contact. Consequences on wear and remediation by a barrel tumble finishing

Manon Isard, Imène Lahouij, Pierre Montmitonnet, Jean-Michel Lanot

Third-body formation by selective transfer in a NiCr / AgPd electrical contact. Consequences on wear and remediation by a barrel tumble finishing

Manon Isard[1,2], Imène Lahouij[1], Pierre Montmitonnet[1] and Jean-Michel Lanot[2]
1. MINES ParisTech, PSL Research University – CEMEF, Centre de Mise en Forme des Matériaux, CNRS UMR7635, Sophia Antipolis, France
2. Vishay S.A, Nice, France

Abstract

The work addresses a particular case of interaction between adhesive and abrasive wear in the electrical contact field, characterized by a selective adhesive transfer layer. The system studied is composed of a resistive element (NiCr thin layer) and a contactor (AgPd), forming an angular position sensor lubricated with a standard silicone oil / PTFE grease. The angular position / electrical resistance relationship is disturbed by wear of the NiCr surfaces, enhanced by the formation on the AgPd contactor of a third body enriched in Ni. From a practical point of view, it has been found that this detrimental Ni-selective transfer formation can be controlled by inserting tumble finishing with lamellar alumina powder as the last step of NiCr track manufacturing. Acting like a solid lubricant, alumina clusters of 1 to 5 µm in size adhere to NiCr surface giving rise to a delay or cancel of Ni adhesion on the contactor which lead to a significant improvement of electrical behavior of the position sensor.

1. Introduction

In electrical components, wear and 3rd body formation have an important impact on the lifetime of the surface contact as well as on the electrical signal quality [1, 2]. Several types of wear phenomena, pertaining to abrasive, adhesive or corrosive wear, may take place in an electrical contact such as:

- Adhesion may block sliding contacts, in particular in microsystems, but it can also enhance wear, resulting in scuffing or seizure and fast degradation of contacting pairs.
- Formation of oxides on surfaces (corrosion) increases contact resistance on the one hand; on the other hand they may reduce wear because of their higher hardness and lower adhesion [3].
- Formation of wear particles deteriorates contact resistance depending on their size and amount; their agglomeration may amplify the phenomena [1].
- Increase of temperatures during sliding movements also impacts contacts, by changing materials properties (softening by Joule heating e.g.) and consequently the coefficient of friction (COF)[1, 4].

In addition, it is known from previous studies that the wear behavior in electrical contact could be affected by the electric current and/or magnetic field which are found in specific cases to enhance electrochemical corrosion and electromigration [5, 6]. Current flow through the contact zone induces changes in the state (characteristics) of surface layers of the contact which can result in large impact on its tribological behavior. Zhang et al. [7] have shown that a current density varying between 1.5 $A.mm^{-2}$ and 2 $A.mm^{-2}$ results in an increase of wear rate and friction of a copper/copper-chromium alloy sliding contact. Moreover, they observed a plastic deformation of the surfaces when electric current was applied due to softening.

Therefore to improve the electric reliability of triboelectric sliding contacts it is essential to get a fundamental understanding of the wear behavior of the mated surfaces which will depend on parameters such as sliding conditions, current density, surface characteristics and in the case of lubricated contacts, the efficiency of the lubricant regarding wear and electrical performances.

This is particularly true when the electric performances of the triboelectric components must remain stable for decades (30 years) as in the present study. The electrical component investigated in this study consists on a position sensor developed for aeronautical applications. The triboelectric contact inside the sensor is composed of:

- a resistive track made out of a Ni-based alloy (NiCr) with a periodic geometry (Fig.1); this particular Ni-based alloy is selected for its electrical resistivity which ensures low sensitivity to temperature.
- a mobile cursor made out of an AgPd alloy, sliding on the track to collect an electrical tension (the applied electrical current is about 1 mA, i.e. 3 $A.mm^{-2}$). The electrical contact is ensured between the curved cursor and track “plateau” (Fig. 1), whereas track “valley” are used as lubricant reservoir and wear particles trap. The contact stress is around 5 MPa.

The electrical contact is lubricated by a silicone oil / PTFE grease deposited on the track/cursor interface. As mentioned previously [2], electrical noise and contact losses can also be caused by the lubricant film. Due to the much higher electrical resistivity of the grease compared to metals, the boundary lubrication regime is mandatory to ensure an electrical contact. If the contact is uniformly covered with a lubricant film, the contact resistance to consider will depend on the lubricant film thickness as shown in eq.(1):

$$R' = \rho_{lubricant} * e_{lubricant}/S_{contact} \quad (1)$$

If we consider the following values:
$\rho_{lubricant} \approx 10^{13}\Omega.m$ (resistivity of the lubricant)
$e_{lubricant}$ = 1 nm (lubricant thickness),
$S_{contact} \approx 0.1\ mm^2$ (contact area).

R’ is estimated to 10^{11} Ω, which is clearly too high compared to the required contact resistance for our component, the total resistance of which is 10^4 Ω. Therefore to ensure adequate electric resistance, several direct contact spots are needed.

However, direct contact between metallic surfaces is known to have an impact on friction behavior and wear rate. The quantity and the efficiency of lubricant in the contact are known to be critical parameters: when a large amount of lubricant enters in the contact, the wear rate decreases [8–13], however this may disturb the electric signal and increase contact resistance. In the electrical contact field, all technologies are based on a compromise between the need of boundary lubrication regime and the necessity to control the wear rate.

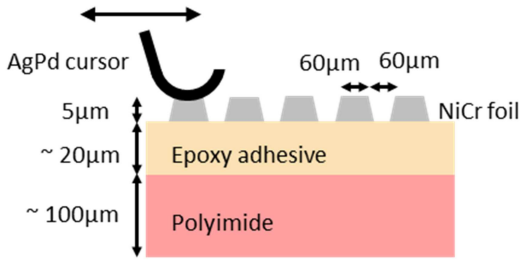

Figure 1: Contact geometry inside the sensor composed by an AgPd cursor in contact with NiCr track. Only a cross section of the coil-shape track is shown.

According to the application of the studied electrical component, an endurance test consisting in ca. 10^5 cycles of low amplitude (vibrations) and large amplitude (actuations) has been applied on all sensors. The results have revealed resistance value drifts and in some cases electrical failures during the lifetime of the sensors. The consequence of the resistance value drift is an offset between the real and the transmitted position-resistance relation.
This study was undertaken with the objective to improve the electrical stability (to attain a resistance value drift under 1%) of the position sensor.

"Passed" endurance tests are mainly characterized by some adhesion of AgPd on NiCr surfaces. Indeed the AgPd cursor is worn during a running-in period, the curved surface turns flat which improves conformity in the contact and stabilizes the real contact stress. AgPd wear particles are transferred to the track (see Fig. 14a) and this also seems to improve electrical contact.
When excessive drifts and/or electrical failure are recorded, severe wear of NiCr surfaces is observed. A first analysis suggests a link between the wear of NiCr surface and the deterioration of the electrical signal quality. This can have two possible origins, either abrasion of the track changing the thickness of the conductor (5 µm initially), or formation of an insulating third body at the interface. Both mechanisms deteriorate surfaces and may decreases electrical conductivity [13, 14].
In the following, the wear mechanisms are investigated together with solutions to improve the tribological properties of the contact. Different parameters could be modified to reach the above objective such as the geometry of the curser and the track in order to minimize stress concentration and severe contact; the lubricant formulation (boundary additives); the lubricant application method and the decrease of the applied normal load. However, these solutions might lead to spurious opening of the circuit. Hence, in this work, we followed another approach which consists on applying a finishing treatment to the NiCr surfaces. The barrel tumble finishing treatment has been used to deburr aggressive surfaces edges, which is known to be efficient against wear [15]. Alumina particles have been added for this purpose. In fact it has been found that alumina forms a patchy deposit on the NiCr track and it has been observed that the results of the electrical endurance test are considerably improved. It has therefore been decided to study the mechanisms behind this improvement of both wear and electric properties.

2. Samples and Materials

The position sensor is composed of a resistive track made out of NiCr alloy (80%Ni 20%Cr), and a mobile cursor out of AgPdCu alloy. These two alloys are hardened by a heat treatment

to prevent wear. The hardness values given by the suppliers of NiCr alloy and AgPd alloy are respectively 430Hv and 270Hv.

The periodic geometry of the track (Fig. 1) is obtained by an electrochemical etching, followed by polishing of a 5 µm thick NiCr foil, which is bonded with epoxy adhesive on a polyimide substrate.

The lubricant is a chlorinated silicone oil / PTFE grease deposited manually on the track/cursor interface at mounting. PTFE is introduced as microspheres (≈2 µm). This lubricant is known to be efficient for electrical contact, because of its chemical inertia, its low volatility and a high resistance to arcing.

3. Experimental Methods

3.1. Endurance tests

An endurance test consisting in ca. 10^5 cycles of back and forth linear movements is applied on all finished parts. The test has been elaborated to reproduce real movements impacting parts during their lifetime, alternating low amplitude vibrations (about 3 mm/ 1 Hz) and large amplitude actuations (about 15 mm/ 0,3 Hz) ; the corresponding average sliding velocities are 6 and 10 $mm.s^{-1}$. The total resistance of the NiCr track is monitored continuously, as well as the signal quality (fluctuation of the transmitted tension).

3.2. Tumble finishing treatment

To improve the contact surfaces, tumble finishing has been applied on NiCr surfaces. It consists in introducing 260 g of glass balls (2 mm diameter), 250 g of distilled water and 3,3 g of alumina powder) in a rotating barrel (effective volume of 3617 cm^3) at a speed of 75 rev/min (7.85 $rad.s^{-1}$), with the tracks glued on its wall. The coverage rate of track surface by adhered Al_2O_3 particles has been measured.
The alumina powder is composed of lamellar particles of 10 nm to 1 µm in size, with a thickness of about 50 nm (Fig. 2).

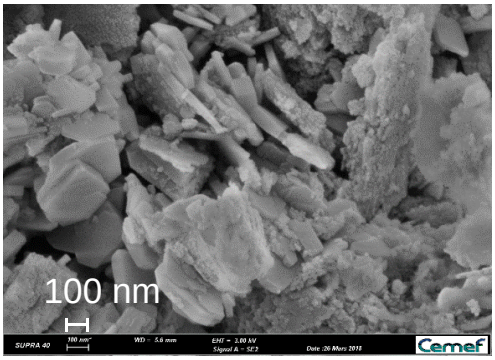

Figure 2: SEM-SE image of alumina powder used for the tumble finishing

3.3 Analytical tools

All samples have been observed and analyzed with Scanning Electron Microscope (SEM) (Philips XL30 and, for high magnification, Zeiss Supra 40), using the SE (Secondary Electron) mode when topography is to be enhanced and the BSE (Backscattered Electrons) mode when chemical contrast is to be enhanced. SEM observations have been coupled with Energy Dispersive X-Ray Spectroscopy (EDS) (Quantax QX400). The analyses were carried out using abeam energy of 15 keV.

To complete EDS analysis, X-Ray Photoelectron Spectrometry has been used (XPS Thermo Scientific K-α system, using a monochromated Al X-Ray source / low energy flood-gun for charge compensation, and an Ar ion gun), in particular to obtain the composition of the third body. The analyzed area is 200 x 400 µm. The energy calibration used the C1s peak at 285 eV. Whenever concentrations are to be calculated, Shirley background subtraction is performed using Alscoof sensitivity factors given by the software Avantage ALTHERMO1.

Indentation tests were performed on NiCr and AgPd samples, to verify the nominal values given by the supplier. *In situ* SEM Indenter platform (Alemnis GmbH, Thun, Switzerland) was used to perform indentation by the side due to the sample shape (only 5 µm thick for NiCr on a soft and non-uniform epoxy/polyimide substrate). A cube corner indenter has been used with a controlled displacement mode (1,5 µm for NiCr and 3 µm for AgPd). Applied loads are a few tens of mN depending on each sample. Hardness (H) values given hereafter are extracted from fitted load-displacement curves using the method of Oliver and Pharr [16], and are averages of about ten indentations for each sample.

Wear profiles have been studied using an optical confocal roughness meter STIL CCS Prima (Chromatic Confocal Sensor), with the MG210 optical detector with a vertical resolution of 3 nm. The displacement step used is 1µm.

4. Behavior of the electrical contact without tumble finishing: Wear and Transfer

4.1 Relationship between wear and electrical resistance

Endurance tests performed on finished parts have displayed resistance drifts and in some cases electrical failures. At the same time, NiCr surfaces are worn with a typical abrasion wear topology: large and deep scratches are observed on NiCr, which are much deeper than pre-existing polishing scratches (see Fig. 7 below).
SEM observations and profiles measurements of NiCr surfaces confirmed that the wear is localized in the contact area between the cursor threads and the track.

The electrical resistance drift can vary in the range of 0 to more than 400 Ω (or 0% to 4% of the full scale). On rare occasions, it can be so high as to cut the circuit (i.e. the 5 µm NiCr layer is worn through). Profiles measurements permit to estimate the wear depth, thus the global loss of material. The formula for the resistance of the resistive track suggests a correlation between wear and resistance drift:

$$R = \rho \frac{L}{S} \quad (2)$$

With R resistance (Ω), ρ resistivity (Ω.m), L length (m) and S=e*w conductive section; e=5 µm is the thickness, w=60 µm the width. Based on formula (2), an increase of 1% of resistance R corresponds to a loss of thickness of 50 nm. The thickness of the NiCr track has an important impact on the resistance value and its drift during endurance tests.

A quantitative link can indeed be evidenced between NiCr layer wear and electrical resistance variations (Fig. 3 and 4). For example, in the case of low resistance drift (64 Ω in Fig. 3a), no reliable estimation of loss of material was obtained, because the wear of NiCr surfaces was negligible. Also with SEM observations, it is difficult to distinguish the worn area from the fresh area.

However, in the case of high resistance drift of 2.57%, the loss of material was estimated of 2.49% (Fig. 3b). Wear tracks are apparent; they have the same dimensions as cursor thread width.

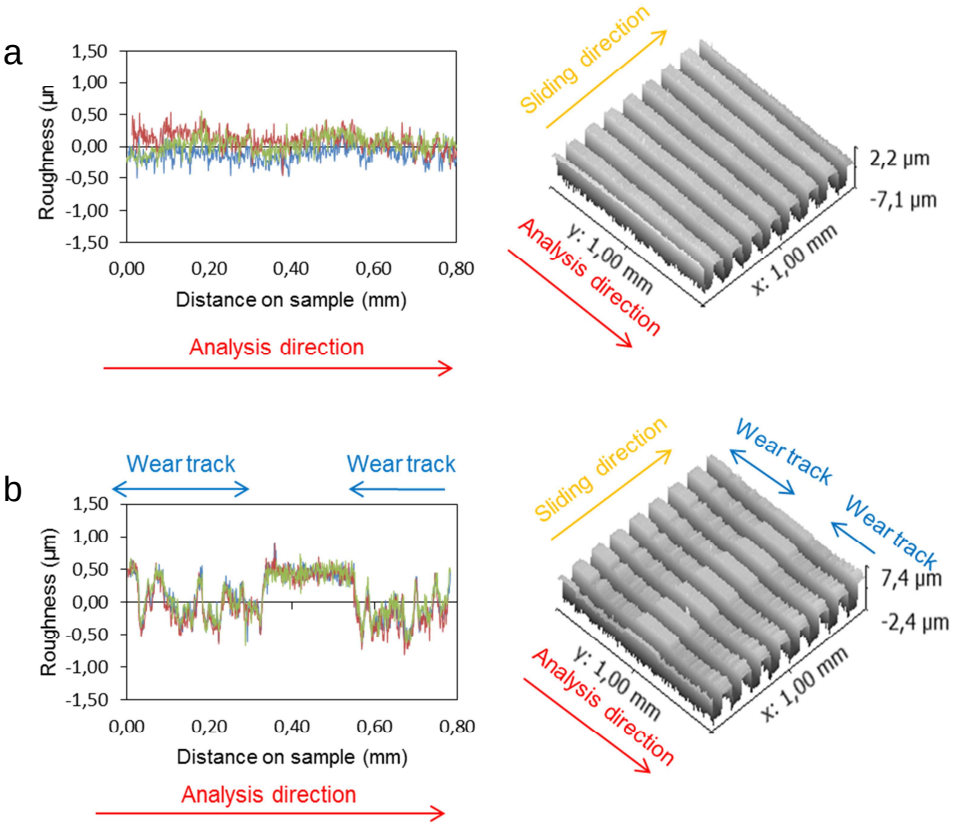

Figure 3: Surface profilometry measurements carried out on an area of 1 mm x 1 mm on the NiCr tracks. (a) From a sensor with a resistance drift of 64 Ω (=0.64%), estimation of wear loss = 0.85%; (b) from a sensor with a resistance drift of 257 Ω (=2.57%), estimation of wear loss = 2.49%

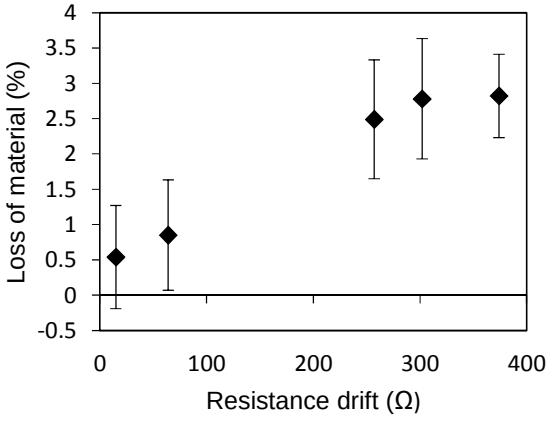

Figure 4: Percentage of material loss estimated from profilometry measurements as a function of the resistance drift recorded at the end of endurance tests carried out on five different sensors

4.2 Wear mechanism: Abrasion

Theoretically, the hardness of NiCr (430 Hv) is higher than that of the AgPd (270 Hv). Therefore, the abrasion wear mode identified previously is unexpected since the supposedly harder material (macroscopically) is worn by the supposedly softer material, which is a paradox to abrasion mechanism: a material scratches another one if it is about at least 1.2 times harder [17].

To verify nominal values of hardness, indentations have been performed on fresh and worn samples of both alloys. For the NiCr sheet, traditional nano-indentation on the surface gave non-reproducible results attributed to the softness and heterogeneity of the glue and the polyimide substrate as well as to the thickness of the NiCr layer (5 µm). It was therefore decided to perform indentation on a cross section (Fig. 5) so as to be less sensitive to this multi-layer character of the track. The *in-situ* indentation ALEMNIS device under SEM imaging allowed this to be done in a reproducible manner. The foil thickness-to-indentation diameter ratio is small (about 2) so that edge effects are to be expected, giving a lower bound of the hardness; but at least the results were reproducible, hence usable. The cursor threads are much thicker and do not raise similar problems.

Figure 5a shows a SEM image of three indentation marks on NiCr sheet. The pile-up behavior is evident around each indentation. This behavior was also observed around the indentations made in the AgPd sample. It is typical of such hardened materials with little residual work-hardening capacity. It is well established that the pile-up effect leads to an increase of the projected contact area which become larger than the cross-sectional area of the indenter at that depth [18,19]. Hence the Oliver-Pharr method may underestimate the real contact area as reported in [19], which leads to an overestimation of Hardness.

In order to evaluate the effect of the pile-up behavior on our measurements, the real contact area of five indents on both alloys were measured directly from the SEM images as reported in [18]. The pile-up factor $C= A_{true}/A_{Oliver\text{-}Pharr}$ describing the ratio of the contact area measured from SEM images (A_{true}) to the contact area estimated by Oliver-Pharr method ($A_{Oliver\text{-}Pharr}$) was then determined for each alloy. This factor is found to be 1.36 ± 0.07 for NiCr and 1.42 ± 0.05 for AgPd. In Figure 6, the values obtained by the Oliver-Pharr method are reported, however it should be noted that due to pile-up effect, both AgPd and NiCr hardness are overestimated by a factor of the order the above-mentioned.
Moreover, the relatively low ratio between the thickness of the NiCr sheet (~5 µm) and the size of the indent marks (~2.6 µm) may give rise to an underestimation of the measured hardness due to geometric artifacts from the edges. Under the indenter, the flow of the material may be boosted by the soft elastic behavior of the surrounding resin. Jakes et al. [20] have shown that the impact of free surface neighborhood is rather pronounced on the modulus, while it is almost insignificant on the hardness for PMMA. In the case of NiCr samples, this artifact is estimated to be around 5-10% for the measured values of hardness.

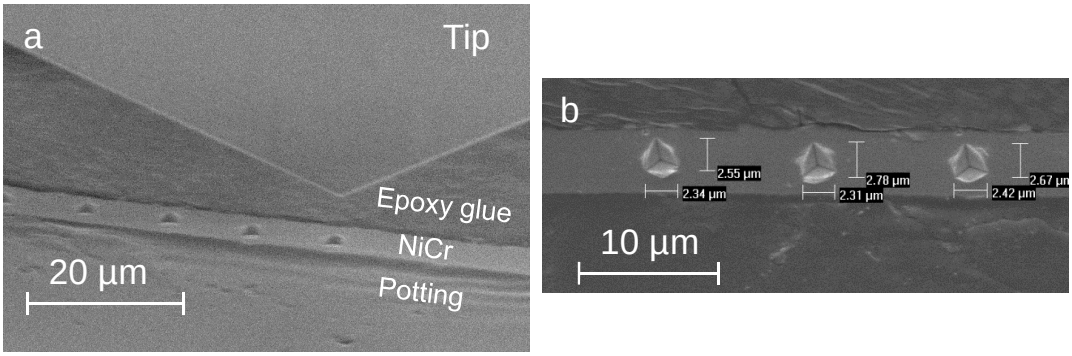

Figure 5: In situ SEM Indentation configuration using ALEMNIS device; (a) Indentation of NiCr tracks by the side; (b) Indentation traces on NiCr showing repeatable dimensions and pile-up behavior.

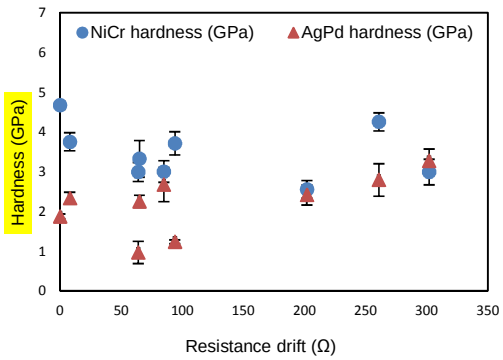

Figure 6: Hardness values estimated using Oliver-Pharr method for each couple track/cursor, represented as a function of the resistance drift recorded for each sensor at the end of endurance test. The data were calculated from displacement-controlled indentation experiments carried out inside a SEM on the cross-section of 5 µm NiCr sheets and AgPd cursors.

Figure 6 shows the hardness values and plots them as the function of the resistance drift measured during endurance tests for eight sensors. From these data, it is clear that the NiCr tracks in general have a higher hardness compared to the AgPd cursors, but the values depart significantly from the nominal ones: some tracks are softer than expected, some cursors are harder. The hardness ratio between the mated surfaces is generally closer to 1 for the sensors having shown larger resistance drift values (Fig. 8). This could explain the abrasion wear of NiCr by AgPd. Moreover, the abrasion could be enhanced by the microstructure of the NiCr and AgPd alloys ("age hardened", "heat treated") which can be composed of hard second phases in a soft matrix.

The AgPd/NiCr hardness ratio shows a global trend, but cannot fully explain the abrasion mechanism taking place on NiCr surfaces. Other observed phenomena have to be analyzed, such as an adhesive 3rd body formation at the interface contact.

4.3. Wear mechanism: adhesion

SEM observations carried out on both NiCr and AgPd surfaces after endurance tests show that whenever NiCr surfaces undergo severe wear, a transfer of material is found on the AgPd surfaces. This third body consists of a transfer of light element (lighter than Ag and Pd) adhered on the AgPd surfaces (Fig. 7 and 8). EDX analysis shows that it is composed of nickel. Moreover, the analyses of the worn surfaces of sensors after endurance tests show a

correlation between the third body formation and the resistance drift value: higher is the resistance drift, more abundant is the transfer of material on the AgPd surface.
In addition, it can be observed in figure 7 some correlation between the adhesive transfer layer morphology on the AgPd cursor and the abrasion scratches on the NiCr tracks. This correlation suggests that the third body contributes to the severe abrasion of the NiCr tracks.

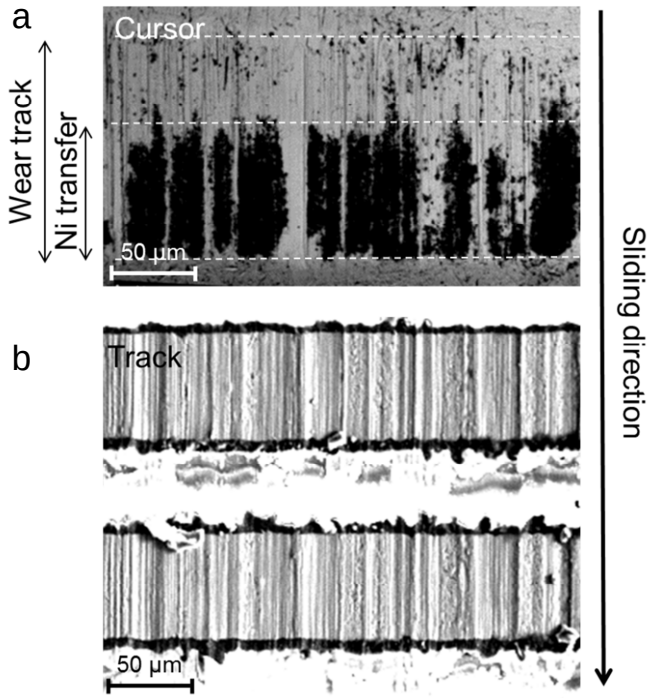

Figure 7: SEM-BSE images of a contact area between the cursor (a) and the NiCr tracks (b) from a sensor with a high resistance drift (257 Ω) after endurance test

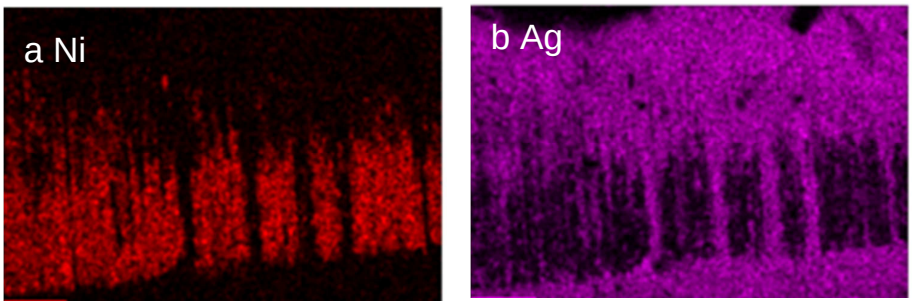

Figure 8: EDS analysis of the contact zone on a cursor, from a sensor with a high resistance drift (257Ω) after endurance test (a) Ni map; (b) Ag map

XPS analyses were performed on a couple of NiCr track and AgPd cursor covered by a transfer layer. Figure 9 shows the Ni2p and Cr2p XPS spectra. Nickel (Ni) and chromium (Cr) are found as expected on the NiCr Track. Concerning the AgPd surface covered by the transfer layer, nickel (Ni) is found as well as silver (Ag) which appears at 573 ev (Fig. 9b). However, chromium (Cr) is not detected on the transfer layer.
Therefore, the transfer layer is identified as selective in nickel and it is expected to change the characteristics of the contact from AgPd-NiCr to Ni-NiCr contact. The severe abrasion taking place at the NiCr track surface suggests this Ni layer is very hard, probably nanocrystalline as a result of intense plastic deformation. Popov et al. [21] have shown that

Ni once work-hardened superficially by severe friction may reach hardness of 5 GPa in the first micrometers of the top surface, which would be sufficient to scratch the NiCr foil.

.

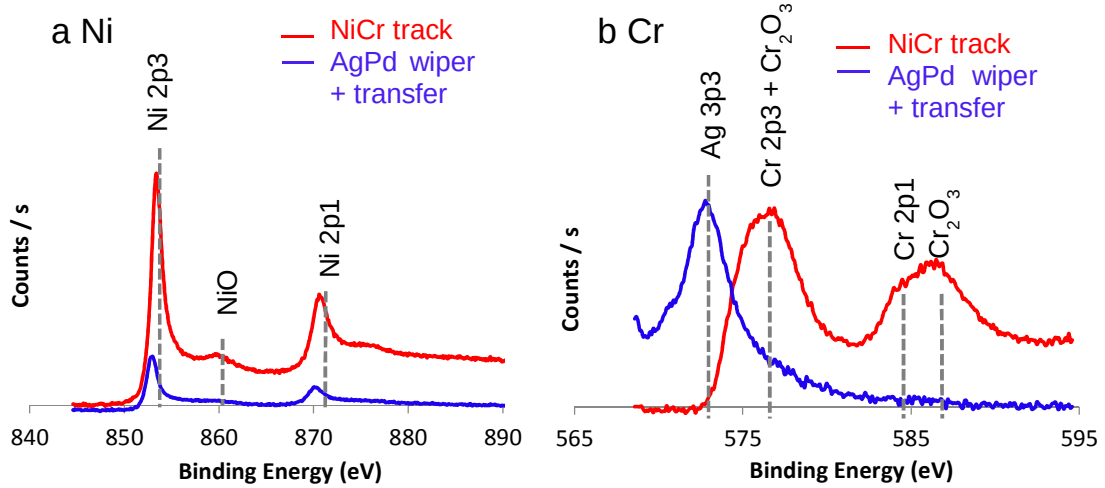

Figure 9: XPS spectra recorded from a AgPd and NiCr contact surfaces with high resistance drift (257Ω) after endurance test, (a) Ni spectrum: Ni is present on NiCr track and on AgPd cursor; (b) Cr spectrum: Cr is present on NiCr track but not on AgPd cursor.

5. Impact of tumble finishing treatment on NiCr surfaces

5.1. Surface state modification

In accordance with the parameters of tumble finishing (low rotation speed, low quantity of glass balls), the indentation tests on NiCr after tumble finishing have not shown any increase in hardness values by strain hardening. Also, no significant modification of polishing scratches of NiCr surface is observed.

However, some particles composed by elements lighter than NiCr adhere on track surfaces and are visible on SEM images (Fig. 10). Using EDS, these particles have been identified as alumina clusters. Other Al_2O_3 particles are dispersed more loosely on the surface (Fig. 10c).

The alumina coverage rate on NiCr surfaces has been estimated by image processing of SEM images with a background subtraction method (Fig. 11). Only the clusters are counted and coverage of 5% is measured.

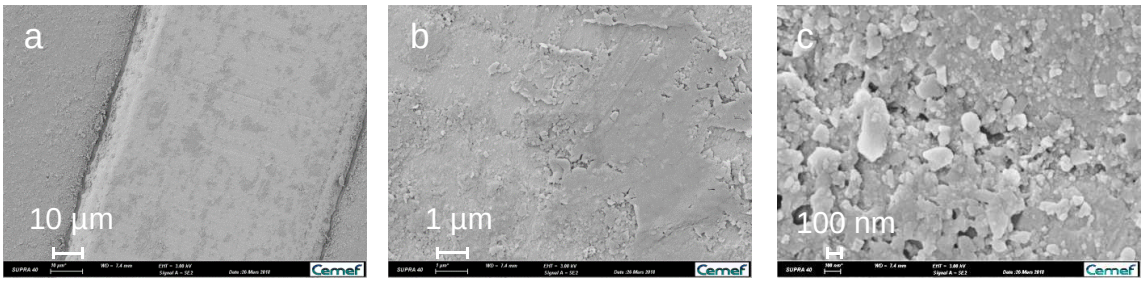

Figure 10: SEM-SE images of NiCr tracks after 30min tumble finishing; (a) at large scale, big alumina clusters are observed (slightly darker grey); (b) an agglomerate of alumina; (c) individual alumina particles

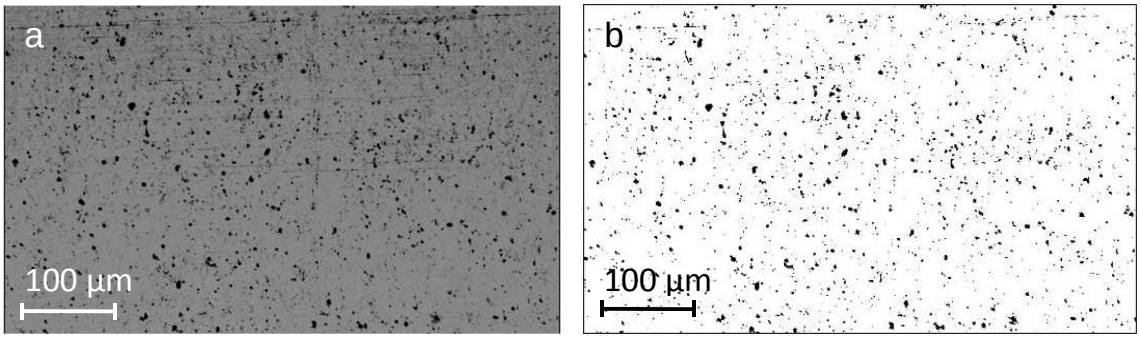

Figure 11: (a) SEM-BSE image of NiCr surface covered by alumina clusters; (b) the corresponding binary image obtained after a background subtraction method (ImageJ)

5.2. Wear behavior and electrical properties of treated NiCr Surfaces

All the endurance tests carried out with treated NiCr tracks show a significant improvement of the resistance drift. While 90% of the endurance tests carried out with sensors equipped with non-treated tracks gave a resistance drift higher than 60 Ω, 100% of sensors equipped with treated NiCr tracks give a resistance drift lower than 60 Ω (Fig. 12).

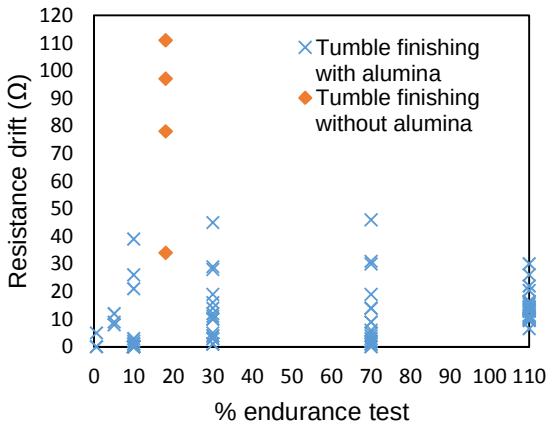

Figure 12: Resistance drifts in Ω, depending on endurance test duration, for different sensors

To check the impact of alumina on this improvement, a tumble finishing without alumina has been carried out (using only glass balls and distilled water). Sensors in this case have the same electrical response than without tumble finishing: the NiCr track shows severe abrasive wear, and the adhesive Ni transfer has been observed on the AgPd cursor (Fig. 13). In addition, high resistance drift values were recorded. In contrast, a tumble finishing with alumina leads to a complete disappearance of adhesive Ni transfer on AgPd cursors. Therefore, tumble finishing is efficient only with the alumina powder; and alumina seems to improve the wear behavior of the contact by avoiding the formation of the adhesive 3rd body.

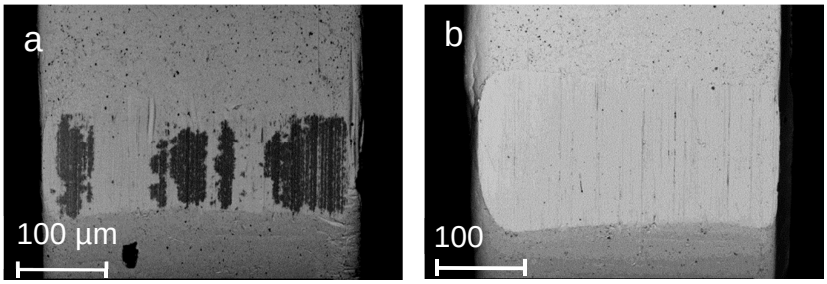

Figure 13: SEM-BSE images of cursor surfaces at the end of endurance tests: (a) the corresponding NiCr surface was treated without alumina; (b) the corresponding NiCr surface was treated with alumina

Partial endurance tests were carried out and stopped at different steps (0,5% , 5% and 110% of the total duty cycle). It must be noted that once dismounted and examined, the sensors cannot be mounted back into the endurance tester so that Fig. 14 shows different sensors from different tests. At the first cycles, the contact seems to be desaligned and the wear takes place only at the left edge of the cursor (Fig. 14a). At this stage the abrasion is accompaned by the formation of third body layer on the most highly loaded area of the AgPd surface, while some of the cursor material is transferred in the other sense (bright lines in BSE images of the NiCr track).

After a 5% endurance test, the cursor wear becomes more homogeneous and the transfer layers grow and cover larger area.

After a 110% endurance test, the third body disappears from the AgPd surface.

Simultaneously, the alumina clusters seem to be moved out from the NiCr contact progressively during the test as shown by EDS analyses carried out inside and ouside the wear track (Fig. 15).

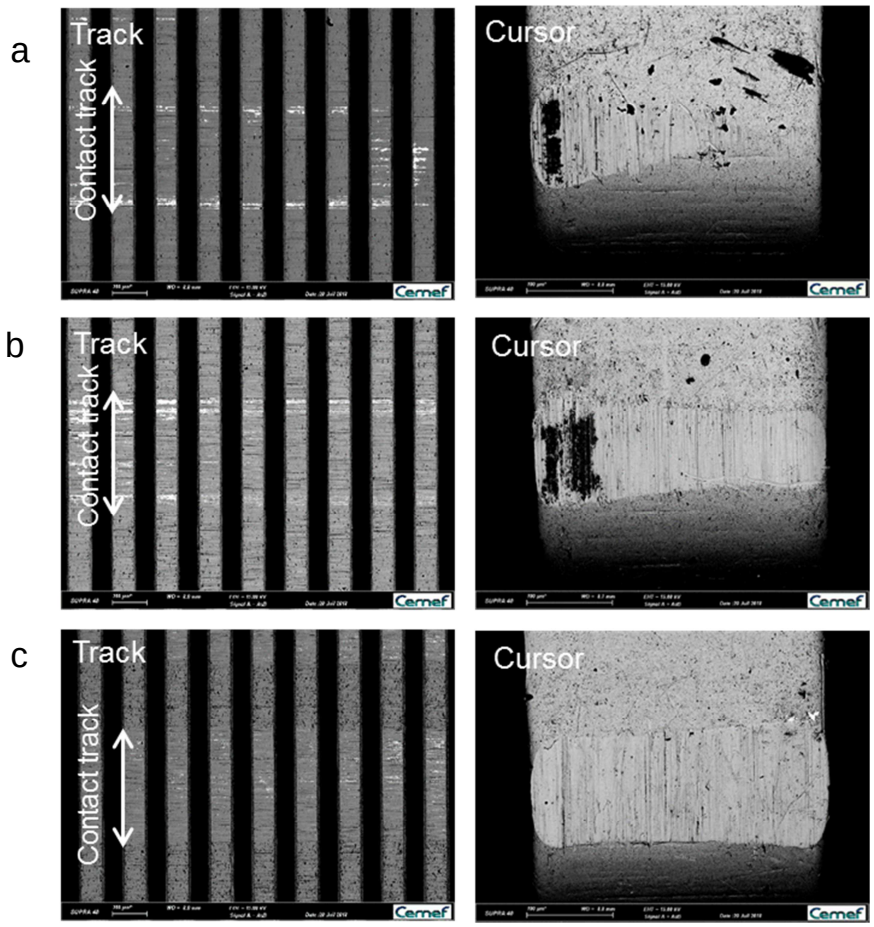

Figure 14: SEM-BSE images of NiCr tracks (left) and AgPd cursors (right) treated by tumble finishing, (a) after 0,5% endurance test; (b) after 5% endurance test; (c) after 110% endurance test

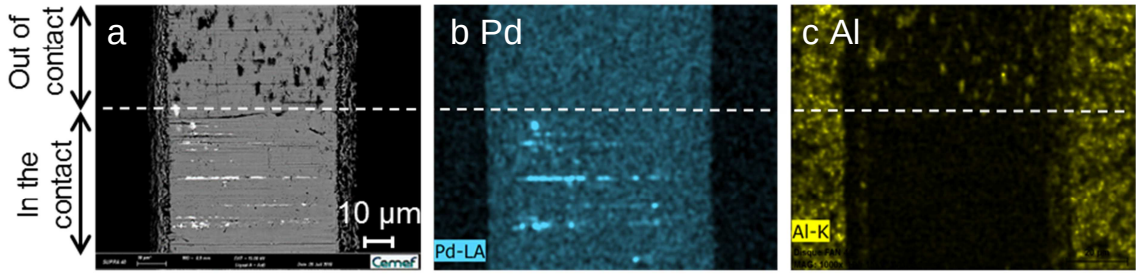

Figure 15: SEM-BSE images of the contact zone from NiCr tracks treated by tumble finishing after 110% endurance test. (a) NiCr track, showing areas inside and outside the contact. (b,c) Pd and Al EDS maps of the NiCr track showed in fig 14, after 110% endurance

6. Discussion

6.1. Formation of the selective transferred Ni layer

The above results clearly show that the high electrical resistance drift recorded during endurance tests is related to the wear mechanisms of the mated surfaces. More specifically, the selective transfer layer rich in nickel observed on the AgPd cursor surfaces is pointed out as the major factor limiting the electrical performances of the contact.

Such a selective transfer has been observed e.g. in high-speed machining where high contact temperatures and high stress gradient accelerate diffusion. Selective transfer can be caused by high temperature in secondary shearing area like in Ti alloy machining with uncoated WC-Co tools [22], which can be simulated by a thermomechanical model of the machining, coupled with a diffusion model [23].
In the present study, heating of the contact is not high enough to cause a selective transfer as in high-speed machining; neither Joule effect nor friction heating could explain a sufficient temperature increase.

Electromigration, i.e. diffusion accelerated by electron shocks on atoms, can also induce a selective transfer to the top surface of conductive elements [24]. Moreover, electrical current and magnetic fields have been shown able to modify the mechanism of formation of the 3rd body, by changing the surface hardness [25, 26].
In the present sensor, no significant magnetic fields are present (intensities are of the order of a mA), and current densities are moderate (a few A/mm^2), so that direct electromagnetic effects are judged improbable.

More work would therefore be needed to explain the formation mechanisms of the third body in the AgPd/NiCr contact.

6.2. Proposed wear mechanisms

Based on the analyses conducted on both non-treated and treated NiCr surfaces, a scenario descripting the wear mechanisms taking place during endurance tests for each case is given below.

After the run-in period during which both surfaces in contact are flattened, the AgPd cursor surface pulls off some Ni particles by an adhesive mechanism. The formation of a thick Ni-rich film on AgPd surface changes the contact nature from NiCr-AgPd to a Ni-NiCr contact, which induces a severe abrasive wear of NiCr tracks. The loss of NiCr material by severe abrasion is the main cause of the increase of electrical resistance drift observed during endurance tests.

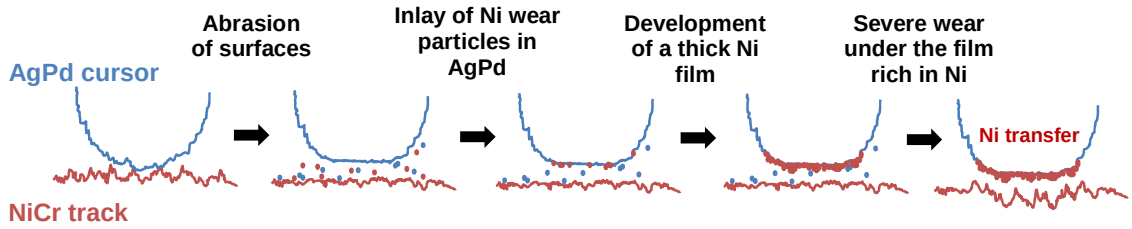

Figure 16: Scenario proposed to describe the wear mechanisms taking place at AgPd/NiCr contact, without tumble finishing.

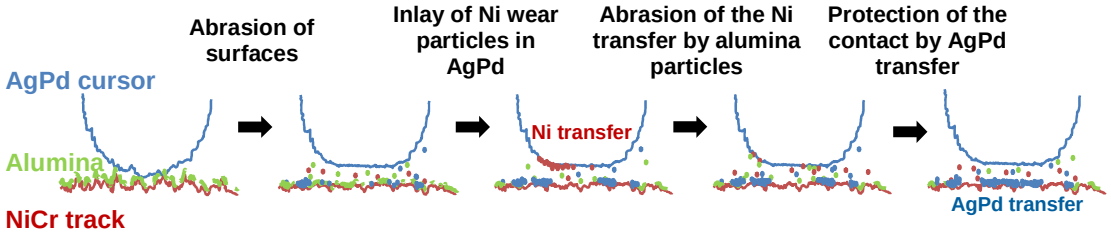

Figure 17: scenario proposed to describe the wear mechanisms taking place at AgPd/NiCr contact, with tumble finishing.

The tumble finishing using alumina powder improves electrical behavior of the sensors. It has been shown that this improvement is related to the role of alumina particles to reduce wear and stop the growth of the Ni transfer layer

Alumina nanoparticles may indeed have a strong impact in contacts [27]. In the automotive industry, alumina nanoparticles have been proposed in engines as a solid additive in lubricants [28]. They could improve anti-wear performance, especially in the boundary lubrication regime, by forming a thin lubricating tribofilm, reducing direct contact between metallic surfaces. Alumina nanoparticles can also have an abrasive action, reducing surface roughness and facilitating the action of other additives [29].

In this study, the coverage of the NiCr surfaces by alumina clusters has an important impact on the wear behavior and improves electrical properties. Alumina clusters do not completely prevent the adhesive Ni transfer on AgPd surface, but make it reversible by an abrasive action (Fig. 17). Alumina clusters seem to be removed progressively from the contact during the endurance tests but this does not lead to a deterioration of electrical contact: it seems that alumina is mainly useful in the running-in stage to prevent fast formation of the deleterious thick Ni transfer layer.

It is expected that the “valleys” of the track play the role of reservoir for alumina particles. Hence a small amount of particles are drained into the contact each time the cursor slides on the track. Some alumina particles are embedded in the grease, and could have the same role as a solid lubricant. It is not possible at this stage to rank this action via the lubricant and the direct action through the initial deposit on the surface.

7. Conclusion

The analysis of the behavior of this tribosystem has disclosed several interesting feature, some usual, others less:

- Electrical behavior degradation is mainly due to wear of the NiCr track rather than e.g. formation of an insulating third body;

- Main wear mode is abrasion, which is caused by the formation of a hard adhesive transfer layer on the counterpart;

- Adhesive transfer shows a selective character with mainly Ni adhering to the noble metal counterpart.

A serendipitous solution has been found in an alumina-assisted tumble finishing processing step added as the last manufacturing stage of the NiCr tracks. It was initially intended to clean the surface asperities which may trigger adhesion. However, this additional treatment step has shown high efficiency against wear through the deposition of lamellar alumina which acts as a solid lubricant during the run-in phase by avoiding the growth of the Ni-rich transfer

layer on the AgPd surface. Moreover, alumina seems to play a role in smoothing the mated surface during the run-in period, which enhances the electric conductivity.

Prospects

- Precise analysis of alumina and its effect on NiCr-AgPd system.
- Improve the tribo-treatment to avoid completely the formation of Ni transfer on AgPd cursor.
- Understand the Ni selective transfer mechanism: role of electric potential and current?
- Analyze the role of lubricant.

Acknowledgement

The authors gratefully acknowledge financial support from the ANRT (CIFRE grant) and from Vishay S.A.

The authors want to thank Fréderic Georgi for his help with XPS analyses, Suzanne Jacomet for her assistance with the SEM analyses and Sylvain Bertrand for his technical assistance with the endurance tests.

References

[1] N. Saka, M. J. Liou, and N. P. Suh, “The role of tribology in electrical contact phenomena,” *Wear*, vol. 100, pp. 77–105, 1984.

[2] M. Antler, “Wear, friction and electrical noise phenomena in severe sliding systems,” *ASLE Trans.*, vol. 5, no. 2, pp. 297–307, 1962.

[3] J. Laporte, S. Fouvry, O. Perrinet, and G. Blondy, “Influence of large periodic sliding sequences on the electronical endurance of contacts subjected to fretting wear,” *Proc. 59th IEEE Holm*, pp. 40–48, 2013.

[4] E. Rabinowicz, “The temperature rise at sliding electrical contacts,” *Wear*, vol. 78, pp. 29–37, 1982.

[5] M. Braunovic, V. V. Konchits, and N. K. Myshkin, *Electrical Contacts□: Fundamentals, Applications and Technology*. 2006.

[6] M. El Mansori, D. Paulmier, GinsztlerJ., and M. Horvath, “Lubrication mechanisms of a sliding contact by simultaneous action of electric current and magnetic field,” *Wear*, pp. 1011–1016, 1999.

[7] Y. Zhang, I. Sun, Y. Chen, and B. Shanggan, “Tribo-electric behaviors of copper under dry sliding against Cu–Cr alloys,” 2004.

[8] E. Querlioz, F. Ville, P. Sainsot, and L. A.A., “Effect of rough surfaces on rolling contact fatigue,” in *STLE Annual Meeting*, 2006.

[9] E. Querlioz, F. Ville, H. Lenon, and T. Lubrecht, “Experimental investigations on the contact fatigue life under starved conditions,” *Tribol. Int.*, vol. 40, no. 10–12, pp. 1619–1626, 2007.

[10] I. Couronné, P. Vergne, D. Mazuyer, N. Truong-Dinh, and D. Girodin, “Effects of Grease Composition and Structure on Film Thickness in Rolling Contact Effects,” *Tribol. Tansactions*, vol. 46, no. 1, pp. 31–36, 2003.

[11] I. Couronné, P. Vergne, D. Mazuyer, N. Truong-Dinh, and D. Girodin, “Nature and Properties of the Lubricating Phase in Grease Lubricated Contact,” *Tribol. Trans.*, vol. 46, no. 1, pp. 37–43, 2003.

[12] T. Cousseau, M. Björling, B. Graça, A. Campos, J. Seabra, and R. Larsson, “Film thickness in a ball-on-disc contact lubricated with greases, bleed oils and base oils,” *Tribol. Int.*, vol. 53, pp. 53–60, 2012.

[13] H. Nagasawa and K. Kato, “Wear mechanism of copper alloy wire sliding against iron-base strip under electric current,” *Wear*, vol. 216, pp. 179–183, 1998.

[14] H. Zhao, G. C. Barber, and J. Liu, “Friction and wear in high speed sliding with and without electrical current,” *Wear*, vol. 249, pp. 409–414, 2001.

[15] F. Salvatore *et al.*, “Experimental and numerical study of media action during tribofinishing in the case of SLM titanium parts,” *Procedia CIRP*, vol. 58, pp. 451 – 456, 2017.

[16] W. C. Oliver and G. M. Pharr, “An improved technique for determining hardness and elastic modulus using load and displacement sensing indentation experiments,” *J.Mater.Res*, vol. 7, no. 6, pp. 1564–1583, 1992.

[17] D. Tabor, “Mohs’ hardness scale - A physical interpretation,” *Proc. Phys. Soc*, vol. B 67, pp. 249–257, 1954.

[18] Y. H. Lee, J. H. Hahn, S. N. Nahm, J. I. Jang, and D. Kwon, “Investigation on indentation size effects using a pile-up corrected hardness,” *J.Phys.D:Appl.Phys.*, vol. 41, no. 74027, 2008.

[19] K. W. McElhaney, J. J. Vlassak, and W. D. Nix, “Determination of indenter tip geometry and indentation contact area for depth-sensing indentation experiments,” *J.Mater.Res.*, vol. 13, no. 5, 1998.
[20] J. E. Jakes *et al.*, “Nanoindentation near the edge,” *J.Mater.Res*, vol. 24, no. 3, pp. 1016–1031, 2009.
[21] I. Popov, A. Moshkovich, S. R. Cohen, V. Perfilyev, A. Vakahy, and L. Rapoport, “Microstructure and nanohardness of Ag and Ni under friction in boundary lubrication,” *Wear*, vol. 404–405, pp. 62–70, 2018.
[22] O. Hatt, P. Crawforth, and M. Jackson, “On the mechanism of tool crater wear during titanium alloy machining,” *Wear*, vol. 374–375, pp. 15–20, 2017.
[23] A. Molinari and M. Nouari, “Modeling of tool wear by diffusion in metal cutting,” *Wear*, vol. 252, pp. 135–149, 2002.
[24] D. A. Golopentia and H. B. Huntington, “A study of electromigration of nickel in lead,” *J. Phys. Chem. Solids*, vol. 39, pp. 975–984, 1978.
[25] M. El Mansori and M. Nouari, “Dry machinability of nickel-based weld-hardfacing layers for hot tooling,” *Int. J. Mach. Tool Manuf.*, vol. 47, pp. 1715–1727, 2007.
[26] M. El Mansori and D. Paulmier, “Effects of selective transfer on friction and wear of magnetised steel–graphite sliding couples,” *Appl. Surf. Sci*, vol. 144–145, pp. 233–237, 1999.
[27] X. Cao *et al.*, “The effect of alumina particle on improving adhesion and wear damage of wheel/rail under wet conditions,” *Wear*, vol. 348–349, pp. 98–115, 2016.
[28] M. K. A. Ali, A. Elagouz, and M. A. A. Abdelkareem, “Minimizing of the boundary friction coefficient in automotive engines using Al2O3 and TiO2 nanoparticles,” *J Nanopart Res*, vol. 18:377, pp. 1–16, 2016.
[29] L. Pena-Paras, J. Taha-Tijerina, and L. Garza, “Effect of CuO and Al2O3 nanoparticle additives on the tribological behavior of fully formulated oils,” *Wear*, vol. 332–333, pp. 1256–1261, 2015.